

## Original Article

# Quantitative measurement of breast carcinoma fibrosis for the prediction in the risk of bone metastasis

Chong Sun<sup>2\*</sup>, Bin Wang<sup>3\*</sup>, Jianmin Li<sup>1</sup>, Junjie Shangguan<sup>3</sup>, Matteo Figini<sup>3</sup>, Kang Zhou<sup>3</sup>, Liang Pan<sup>3</sup>, Quanhong Ma<sup>3</sup>, Zhuoli Zhang<sup>3,4</sup>

<sup>1</sup>Department of Orthopedics, Qilu Hospital, Shandong University, Jinan, Shandong, China; <sup>2</sup>Department of Orthopedics, The Affiliated Hospital of Qingdao University, Qingdao, Shandong, China; <sup>3</sup>Department of Radiology, Feinberg School of Medicine, Northwestern University, Chicago, IL, USA; <sup>4</sup>Robert H. Lurie Comprehensive Cancer Center, Chicago, IL, USA. \*Equal contributors.

Received February 5, 2018; Accepted May 6, 2018; Epub June 15, 2018; Published June 30, 2018

**Abstract:** Background: Previous studies have shown the poor prognosis of metastatic breast cancer including bone metastasis. The early prediction and intervention of invasive breast carcinoma with bone metastasis are crucial to the outcomes of patients. The purpose of our study is to test the hypothesis that the collagen deposition of primary breast cancer can be used as a quantitative biomarker for the early prediction of bone metastasis. Methods: A total of sixty breast cancer patients were included in our study, and the surgical specimens of these patients were divided into three groups: patients with no metastasis (group 1), lymph node metastasis (group 2), and bone metastasis (group 3). Masson's trichrome staining and hematoxylin and eosin staining were applied to all primary breast cancers. Collagen area percentage and tumor cell measurement of each sample were measured by HistoQuest software. Results: Measurement results of collagen area percentage (%) in primary breast tumors were  $32.39 \pm 13.30$ ,  $25.37 \pm 11.10$ , and  $22.71 \pm 8.91$  for groups 1, 2, and 3, respectively. The corresponding *P* values were 0.0779 (group 1 vs. group 2), 0.4086 (group 2 vs. group 3), and 0.0102 (group 1 vs. group 3). The correlation between collagen area percentage and tumor cell measurement were group 1 (*P* = 0.5927, *r* = -0.1273), group 2 (*P* = 0.5711, *r* = -0.1348), and group 3 (*P* = 0.0003, *r* = -0.7253). Conclusions: The collagen deposition of primary breast cancer can be used as a quantitative biomarker for the early prediction of bone metastasis.

**Keywords:** Invasive breast carcinoma, bone metastasis, collagen deposition, early prediction

## Introduction

Breast cancer (BC) is the most common cancer among females worldwide [1, 2]. In China, due to the increase of risk factors associated with changing lifestyles, BC rates increase in recent years. The total mortality was estimated to be 70.7 thousand [3]. Approximately 30% of women initially diagnosed with early-stage BC will ultimately develop metastatic lesions, often months or even years later [4, 5]. BC mainly metastasizes to regional lymph node, skeleton system, lungs, liver, and brain via the circulation [6]. A study of total 784 metastatic breast cancer (mBC) patients showed that axillary lymph node metastases occurred in 520 patients (66.3%), and the common involved distant organs were as follows: bone metastases in 374 patients (47.7%), liver metastases in

239 patients (30.5%), lung metastases in 201 patients (25.6%), and brain metastases in 54 patients (6.9%) [7].

The skeleton is a common site for metastases from BC, and it is often associated with progressive debility. Patients with bone metastases are vulnerable to complications or skeletal-related events (SREs), defined as fracture, spinal cord compression, and surgery or radiation to bone. Aside from the large amount health care costs, the SREs also have a significant impact on overall quality of life, and the occurrence of SREs is associated with worse survival as well. Radiation and systemic therapies may be used, but just for palliation of pain in these patients [8]. Thus, it is very important to predict bone metastases at an early stage to minimize SREs and to prolong survival time after the initial diagnosis.

## Breast cancer fibrosis and bone metastasis

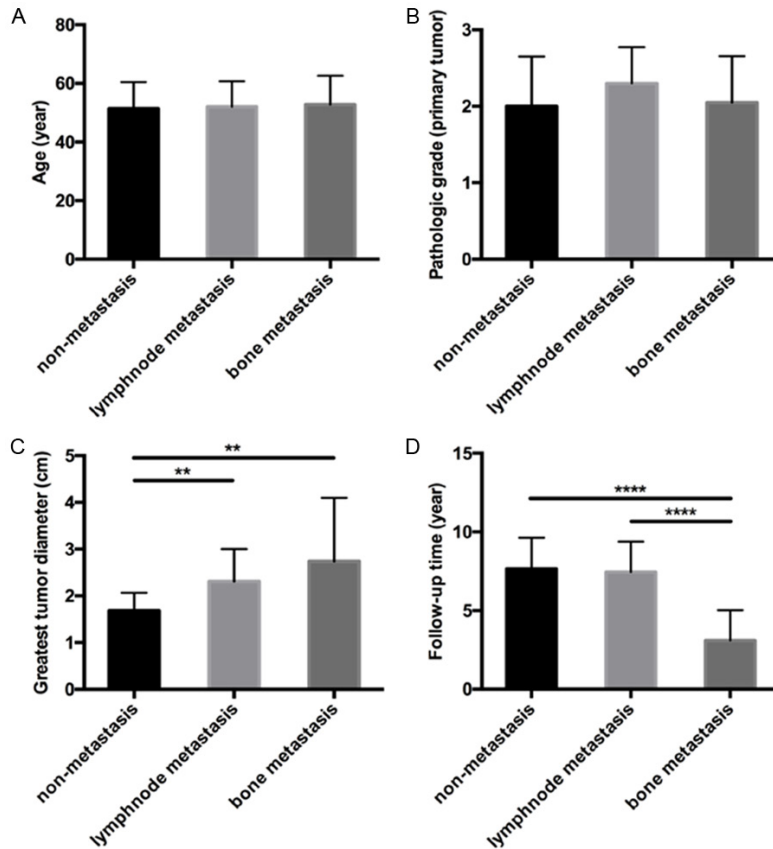


**Figure 1.** Clinical information of the three groups of patients (non-metastasis, lymph node metastasis, and bone metastasis): age (A), pathologic grade (B), greatest tumor diameter (C), and follow-up time (D).

The purpose of our study is to test the hypothesis that the collagen deposition of primary breast cancer can be used as a quantitative biomarker for the early prediction of bone metastasis.

### Materials and methods

#### Collecting of surgical specimens

This retrospective study of pathological samples was approved by the institutional review board of Shandong university, and the informed consent was obtained from all patients. Sixty patients having primary invasive breast carcinoma were included in this study. All the paraffin-embedded surgical specimens of the primary breast tumor were acquired from patients of Qilu hospital, Shandong university between 2009 and 2014. The primary invasive breast carcinoma dissections and regional lymph node dissections were carried out among all these 60 patients. All patients' paraffin-embed-

ded tissue blocks containing the primary breast tumor and their original medical records were attainable for the purpose of follow up studies. Specimens were collected from BC patients without any lymph node and other site metastasis (group 1; n = 20), with only lymph node metastases (group 2; n = 20), or with bone metastases (group 3; n = 20). All the medical reports pertaining to clinical pathological characteristics of these patients were retrieved from the department of pathology. Clinical information, for example, the primary tumor size, lymph node metastasis status, distant metastasis status, and the histological grade of these invasive breast carcinomas, were recorded. The pathological tumor-node-metastasis (pTNM) classification system (International Union against Cancer) was applied to identify the stages of these invasive breast carcinomas.

#### Hematoxylin and eosin (HE) staining, Masson's trichrome staining, and histologic evaluation

All the paraffin-embedded surgical specimens of the primary breast tumor were trimmed using a microtome, and then cut into 5  $\mu\text{m}$  slices [9, 10]. The slides were submitted to the pathology core for HE staining and Masson's trichrome staining [11-14]. The HE and trichrome staining were carried out in the same batch for all the samples.

To quantify the amount of fibrosis in each BC primary tumor, the area of collagen in each tumor trichrome-stained slice was measured and compared with the overall tumor area. Specifically, trichrome-stained slides were scanned at 10 $\times$  magnification and digitized using the TissueFAXS system (TissueGnostics, Los Angeles, CA, USA) [15, 16]. Next the acquired images were analyzed using HistoQuest cell analysis software (TissueGnostics) for the automated measurement of the collagen tissue

## Breast cancer fibrosis and bone metastasis

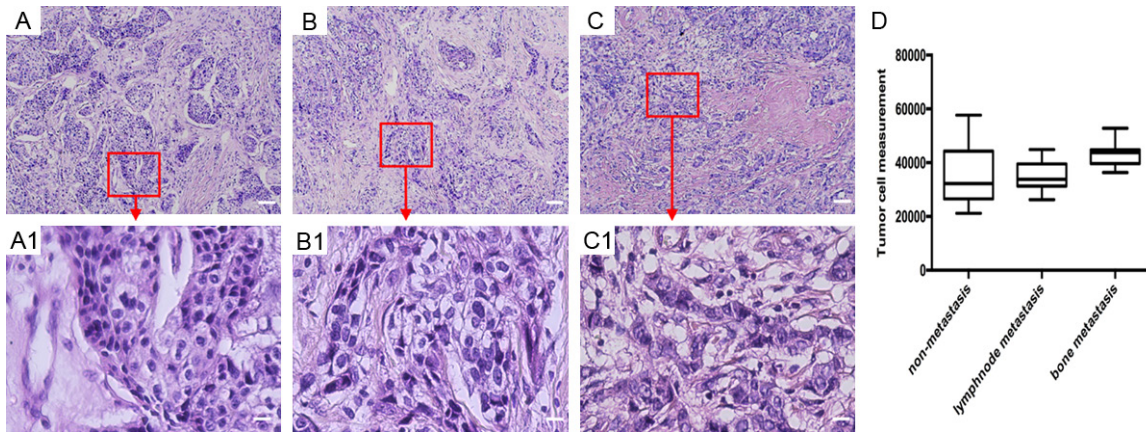


**Figure 2.** (A-C) Representative HE images of patients with no metastasis (A), lymph node metastasis (B), and bone metastasis (C). Scale bar indicates 100  $\mu$ m. (A1-C1) Magnified images of typical areas from patients with no metastasis (A1), lymph node metastasis (B1), and bone metastasis (C1). Scale bar indicates 25  $\mu$ m. (D) Tumor cell measurement result of the three groups of patients (non-metastasis, lymph node metastasis, and bone metastasis), the corresponding *P* values: *P* = 0.8048 (group 1 vs. group 2); *P* < 0.0001 (group 2 vs. group 3); *P* = 0.0081 (group 1 vs. group 3).

area within each slide. The same threshold was used for all samples to segment distinct blue-stained areas for automated identification as collagen tissue. The total tumor tissue area was measured as well. The percentage of collagen tissue was expressed as a percentage of collagen area/total tumor area [17].

For tumor cell measurement, the digital HE slides were imported into the HistoQuest software, and the same threshold was used for all samples to segment distinct “nuclear” for automated identification of tumor cells. The threshold of the staining mean intensity and cut-off value were determined after the multiple tests, and the unattended analysis was carried out automatically [18, 19]. The region of interest (ROI) area of each slide was six square millimeters.

### Statistical analyses

The statistical calculations were performed with software SPSS version 23 (IBM, New York, USA). Data were presented as mean  $\pm$  standard deviation (SD). The unpaired student's *t*-test was used to test the relevant variables, such as the collagen area percentage and the tumor cell measurement. Pearson correlation coefficients were calculated to assess the relationship between collagen area percentage and tumor cell measurement. *P* < 0.05 was considered to indicate a statistically significant difference.

### Results

There was no significant difference in age and tumor pathologic grade among the three groups of patients. The significant difference of the greatest tumor diameter was observed between group 1 and group 2, between group 1 and group 3, but not between group 2 and group 3. Besides, the significant difference of the follow-up time existed between group 1 and group 3, between group 2 and group 3, but not between group 1 and group 2, which were conformed to the expectation since patients with bone metastases always lived a shorter period of time than those with or without lymph node metastases. All clinical information described above was shown in **Figure 1**. Pathological results showed that forty-seven patients had infiltrating ductal carcinoma, seven patients had infiltrating lobular carcinoma, three patients had infiltrating mucinous carcinoma, two patients had basaloid carcinoma, and one patient had invasive tubular carcinoma.

Invasive ductal carcinoma is the most common type of breast cancer. About 80% of all breast cancers are invasive ductal carcinomas. Three representative HE stained images (TissueFAXS) from group 1, group 2 and group 3 were shown in **Figure 2A-C**, and the corresponding magnified images of some areas were shown with arrows in **Figure 2A1-C1**. There was no prominent tubule formation or small round nuclei in these three groups. The group 1 and group 2

## Breast cancer fibrosis and bone metastasis

**Table 1.** Histologic characteristics of 60 breast cancer patients (in accordance with the metastatic status)

Characteristics	Group 1	Group 2	Group 3	P value (group 1 vs. group 2)	P value (group 2 vs. group 3)	P value (group 1 vs. group 3)
Masson's staining ROI area (mm <sup>2</sup> )	27.32 ± 9.67 (27.09, 10.51-47.30)	46.36 ± 12.64 (51.36, 18.90-61.69)	40.71 ± 14.85 (39.15, 18.51-72.87)	< 0.0001	0.2033	0.0017
Collagen area (mm <sup>2</sup> )	8.90 ± 4.84 (8.40, 1.74-21.24)	11.62 ± 5.43 (11.13, 2.39-22.01)	9.28 ± 4.78 (8.64, 2.05-17.98)	0.1036	0.1573	0.8047
Collagen area percentage (%)	32.39 ± 13.30 (31.00, 9.98-54.77)	25.37 ± 11.10 (24.98, 10.01-52.19)	22.71 ± 8.91 (24.27, 5.03-34.29)	0.0779	0.4086	0.0102
Tumor cell measurement (six mm <sup>2</sup> )	35661.95 ± 10966.80 (32263.00, 21169.00-57675.00)	34979.90 ± 5472.62 (33782.50, 26151.00-44830.00)	43010.85 ± 4234.56 (43676.50, 36368.00-52802.00)	0.8048	< 0.0001	0.0081

SD (Standard deviation); ROI (Region of interest).



## Breast cancer fibrosis and bone metastasis

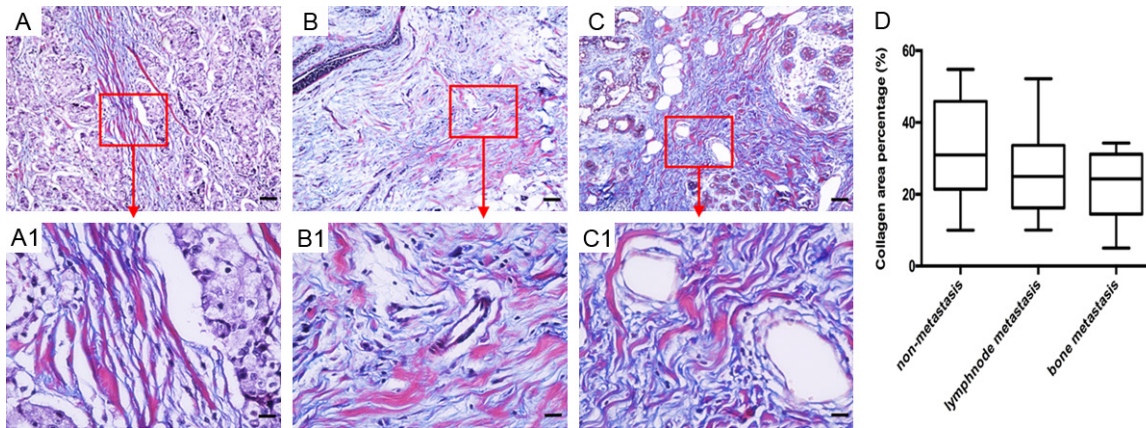


**Figure 3.** (A-C) Representative Masson's trichrome stained images of patients with no metastasis (A), lymph node metastasis (B), and bone metastasis (C). Scale bar indicates 100  $\mu$ m. (A1-C1) Magnified images of specific collagen fiber areas from patients with no metastasis (A1), lymph node metastasis (B1), and bone metastasis (C1). Scale bar indicates 25  $\mu$ m. (D) Collagen area percentage (%) result of the non-metastasis group, lymph node metastasis group, and bone metastasis group; the corresponding *P* values: *P* = 0.0779 (group 1 vs. group 2), *P* = 0.4086 (group 2 vs. group 3), and *P* = 0.0102 (group 1 vs. group 3).

had solid tumor cell clusters and single infiltrating tumor cells as well as the nuclear pleomorphism and mitotic figures, which were the manifestation of moderately differentiated carcinoma. For group 3, the image contained ragged nests or solid sheets of tumor cells with enlarged irregular nuclei, tumor necrosis, a greater degree of nuclear pleomorphism and more mitotic figures, which were the presentation of poorly differentiated carcinoma.

The quantitative tumor cell measurement was conducted automatically using HistoQuest software (Version 4.0.4.168) [18, 19], and the results were shown in **Table 1**. There were  $35661.95 \pm 10966.80$  (median, 32263.00; range, 21169.00 to 57675.00),  $34979.90 \pm 5472.62$  (median, 33782.50; range, 26151.00 to 44830.00), and  $43010.85 \pm 4234.56$  (median, 43676.50; range, 36368.00 to 52802.00) in group 1, group 2, and group 3, respectively. The tumor cell measurement was calculated by the amount of tumor cell nucleus, and the corresponding results were summarized as a box plot (**Figure 2D**). There was significant difference between group 1 and group 3 (*P* = 0.0081), between group 2 and group 3 (*P* < 0.0001), but not between group 1 and group 2 (*P* = 0.8048).

Three representative Masson's trichrome stained images are from group 1, group 2, and group 3 in **Figure 3A-C**. The corresponding magnified images in **Figure 3A1-C1** showed

that the collagen shape of invasive breast carcinoma had a large variety, which could be described as straight, intermediate, and curly. The sample area and collagen area were measured by HistoQuest software (Version 4.0.4.168), and the collagen area percentage was calculated. The quantitative measurement results of the ROI area ( $\text{mm}^2$ ) were shown in **Table 1**. The corresponding results were  $27.32 \pm 9.67$  (median, 27.09; range, 10.51 to 47.30),  $46.36 \pm 12.64$  (median, 51.36; range, 18.90 to 61.69), and  $40.71 \pm 14.85$  (median, 39.15; range, 18.51 to 72.87) for groups 1, 2, and 3, respectively. There was significant difference between group 1 and group 2 (*P* < 0.0001), between group 1 and group 3 (*P* = 0.0017), but the significant difference was not observed between group 2 and group 3 (*P* = 0.2033). The results of the distinct blue-stained collagen area ( $\text{mm}^2$ ) were  $8.90 \pm 4.84$  (median, 8.40; range, 1.74 to 21.24),  $11.62 \pm 5.43$  (median, 11.13; range, 2.39 to 22.01), and  $9.28 \pm 4.78$  (median, 8.64; range, 2.05 to 17.98) for group 1, group 2, and group 3, respectively. There was no significant difference between groups for the collagen area. Measurement of collagen area percentage (%) for groups 1, 2, and 3 were  $32.39 \pm 13.30$  (median, 31.00; range, 9.98 to 54.77),  $25.37 \pm 11.10$  (median, 24.98; range, 10.01 to 52.19), and  $22.71 \pm 8.91$  (median, 24.27; range, 5.03 to 34.29), respectively. A descending trend from group 1 to group 3 was observed in the results (**Figure 3D**). The signifi-

## Breast cancer fibrosis and bone metastasis

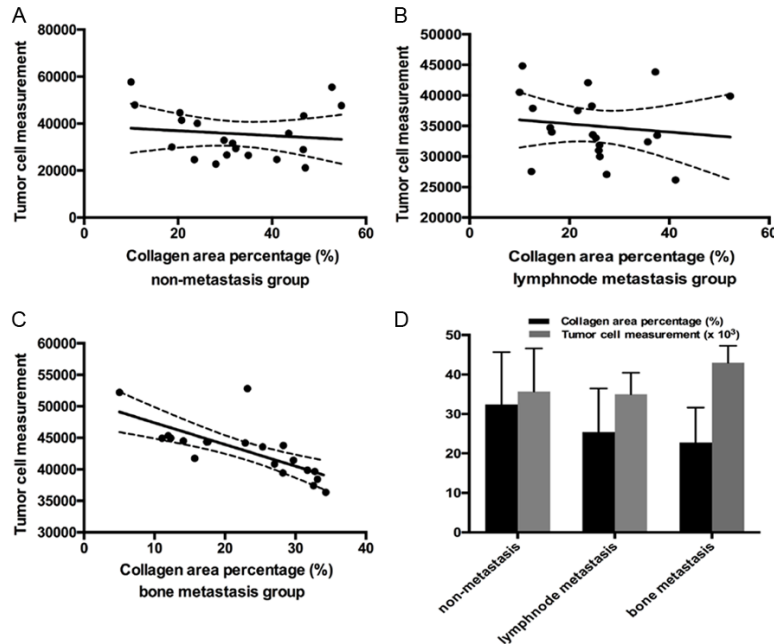


**Figure 4.** (A-C) Correlation between collagen area percentage (%) and tumor cell measurement for the patients with no metastasis (A), lymph node metastasis (B), and bone metastasis (C); the corresponding statistical results: non-metastasis group ( $P = 0.5927$ ,  $r = -0.1273$ ), lymph node metastasis group ( $P = 0.5711$ ,  $r = -0.1348$ ), and bone metastasis group ( $P = 0.0003$ ,  $r = -0.7253$ ). (D) The trend existing in the results of collagen area percentage and tumor cell measurement from the non-metastasis group through lymph node metastasis group to bone metastasis group.

cant difference existed between group 1 and group 3 ( $P = 0.0102$ ), but not between group 1 and group 2 ( $P = 0.0779$ ), or between group 2 and group 3 ( $P = 0.4086$ ).

To find out the correlation between collagen area percentage and tumor cell measurement, we used the Pearson correlation analysis for each group of patients. The corresponding results ( $r$  value) for groups 1, 2, and 3 were  $-0.1273$ ,  $-0.1348$ , and  $-0.7253$ , respectively (Figure 4A-C). There was significance in group 3 ( $P = 0.0003$ ), but not in group 1 ( $P = 0.5927$ ) or group 2 ( $P = 0.5711$ ). Furthermore, the comparison diagram of collagen area percentage and tumor cell measurement was used as Figure 4D to show the trend of these two parameters.

### Discussion

The progression of breast cancer is significantly influenced by its surrounding stromal tissue. Particularly, collagen fibers in tumor-adjacent stroma affect tumor growth and metastasis

[20-22]. In our study, we investigated the relationship between the relative content of collagen in early stage invasive breast carcinoma specimen and the long-term occurrence of bone metastasis by using the Masson's trichrome staining technique. To reduce bias, the collagen area percentage was used in the study. Our study shows that a strong correlation exists between the collagen component of early stage breast carcinoma and the later occurrence of bone metastasis. Moreover, strong correlation between collagen area percentage and tumor cell measurement was observed in each group of patients.

There were two contradictory viewpoints towards the relationship between human BC progression and collagen deposition. Previous study showed that BC stroma contained less collagen deposi-

tion compared with the normal breast tissue, but this was not included in our study since the investigation of normal breast tissue could not be approved by our institutional review board [23]. A large variety of shapes of collagen structure in the three groups of invasive breast carcinoma were found in our study, which were also reported by previous report [24].

Other studies showed a contrary opinion. In a transgenic mouse model study, results demonstrated that the increased collagen density can promote the tumorigenesis, local invasion, and metastasis in mouse mammary tumor, and this indicated that the tumor formation and progression was closely associated with the increased stromal collagen deposition [25]. Another study also showed the correlation between collagen content and malignant progression of BC using human breast tissue samples [26]. By quantifying the samples of invasive ductal carcinoma, ductal carcinoma in situ, and adjacent normal tissue, they found that the collagen content increased from normal tissue through ductal carcinoma in situ to invasive ductal carcino-

## Breast cancer fibrosis and bone metastasis

ma in the trichrome stained samples. Given the existence of these two contrary conclusions discussed above, further studies need to be conducted because the correlation between collagen deposition and bone metastasis has a critical impact on the early prediction and effective treatment of the invasive breast cancer patients.

There were two main limitations consisting in our study. First, the sample size of this study was comparatively small, and it may not be big enough to reflect the overall situation. But, to the best of our knowledge, there was no similar research in human invasive breast carcinoma. Second, there was no significant correlation between collagen area percentage and tumor cell measurement in group 1 and group 2. More studies with a larger sample size will be performed to better verify the correlation between collagen content and bone metastasis, and between collagen content and tumor cell measurement.

### Conclusion

The collagen deposition of primary breast cancer can be used as a quantitative biomarker for the early prediction of bone metastasis.

### Acknowledgements

This research was generously supported by NIH NCI R01CA196967 and NIH NCI R01CA209886.

Informed consent was obtained from all individual participants included in the study.

### Disclosure of conflict of interest

None.

### Abbreviations

BC, Breast cancer; mBC, Metastatic breast cancer; SREs, Skeletal-related events; pTNM, Pathological tumor-node-metastasis; HE, Hematoxylin and eosin; ROI, Region of interest; SD, Standard deviation.

**Address correspondence to:** Jianmin Li, Department of Orthopedics, Qilu Hospital, Shandong University, Jinan, Shandong, China. Tel: +86 18560082577; E-mail: sddxqllyljm@163.com; Zhuoli Zhang, Department of Radiology, Robert H. Lurie Comprehensive Cancer Center Northwestern University, 737 N. Michigan Ave, 16th Floor, Chicago, IL 60611. Tel:

312-926-3874; Fax: 312-926-5991; E-mail: zhuoli-zhang@northwestern.edu

### References

- [1] Torre LA, Bray F, Siegel RL, Ferlay J, Lortet-Tieulent J and Jemal A. Global cancer statistics, 2012. *CA Cancer J Clin* 2015; 65: 87-108.
- [2] Global Burden of Disease Cancer Collaboration, Fitzmaurice C, Allen C, Barber RM, Barre-gard L, Bhutta ZA, Brenner H, Dicker DJ, Chimed-Orchir O, Dandona R, Dandona L, Fleming T, Forouzanfar MH, Hancock J, Hay RJ, Hunter-Merrill R, Huynh C, Hosgood HD, Johnson CO, Jonas JB, Khubchandani J, Kumar GA, Kutz M, Lan Q, Larson HJ, Liang X, Lim SS, Lopez AD, MacIntyre MF, Marczak L, Marquez N, Mokdad AH, Pinho C, Pourmalek F, Salomon JA, Sanabria JR, Sandar L, Sartorius B, Schwartz SM, Shackelford KA, Shibuya K, Stanaway J, Steiner C, Sun J, Takahashi K, Vollset SE, Vos T, Wagner JA, Wang H, Westerman R, Zeeb H, Zockler L, Abd-Allah F, Ahmed MB, Alabed S, Alam NK, Aldhahri SF, Alem G, Alemayohu MA, Ali R, Al-Raddadi R, Amare A, Amoako Y, Artaman A, Asayesh H, Atnaflu N, Awasthi A, Saleem HB, Barac A, Bedi N, Bensenor I, Berhane A, Bernabe E, Betsu B, Binagwaho A, Boneya D, Campos-Nonato I, Castaneda-Orjuela C, Catala-Lopez F, Chiang P, Chibueze C, Chittheer A, Choi JY, Cowie B, Damtew S, das Neves J, Dey S, Dharmaratne S, Dhillon P, Ding E, Driscoll T, Ekwueme D, Endries AY, Farvid M, Farzadfar F, Fernandes J, Fischer F, G/Hiwot TT, Gebru A, Gopalani S, Hailu A, Horino M, Horita N, Hussein A, Huybrechts I, Inoue M, Islami F, Jakovljevic M, James S, Javanbakht M, Jee SH, Kasaeian A, Kedir MS, Khader YS, Khang YH, Kim D, Leigh J, Linn S, Lunevicius R, El Razek HMA, Malekzadeh R, Malta DC, Marcenes W, Markos D, Melaku YA, Meles KG, Mendoza W, Mengiste DT, Meretoja TJ, Miller TR, Mohammad KA, Mohammadi A, Mohammed S, Moradi-Lakeh M, Nagel G, Nand D, Le Nguyen Q, Nolte S, Ogbo FA, Oladimeji KE, Oren E, Pa M, Park EK, Pereira DM, Plass D, Qorbani M, Radfar A, Rafay A, Rahman M, Rana SM, Soreide K, Satpathy M, Sawhney M, Sepanlou SG, Shaikh MA, She J, Shiue I, Shore HR, Shrimel MG, So S, Soneji S, Stathopoulou V, Stroumpoulis K, Sufiyan MB, Sykes BL, Tabares-Seisdedos R, Tadese F, Tedla BA, Tessema GA, Thakur JS, Tran BX, Ukwaja KN, Uzochukwu BSC, Vlassov VV, Weiderpass E, Wubshet Terefe M, Yebo HG, Yimam HH, Yonemoto N, Younis MZ, Yu C, Zaidi Z, Zaki MES, Zenebe ZM, Murray CJL and Naghavi M. Global, regional, and national cancer incidence, mortality, years of life lost, years lived with disability, and disability-adjusted life-years for 32 cancer groups, 1990 to 2015: a



## Breast cancer fibrosis and bone metastasis

- systematic analysis for the global burden of disease study. *JAMA Oncol* 2017; 3: 524-548.
- [3] Chen W, Zheng R, Baade PD, Zhang S, Zeng H, Bray F, Jemal A, Yu XQ and He J. Cancer statistics in China, 2015. *CA Cancer J Clin* 2016; 66: 115-132.
- [4] Sundquist M, Brudin L and Tejler G. Improved survival in metastatic breast cancer 1985-2016. *Breast* 2017; 31: 46-50.
- [5] DeSantis CE, Fedewa SA, Goding Sauer A, Kramer JL, Smith RA and Jemal A. Breast cancer statistics, 2015: convergence of incidence rates between black and white women. *CA Cancer J Clin* 2016; 66: 31-42.
- [6] Nola S, Sin S, Bonin F, Lidereau R and Driouch K. A methodological approach to unravel organ-specific breast cancer metastasis. *J Mammary Gland Biol Neoplasia* 2012; 17: 135-145.
- [7] Hess KR, Varadhachary GR, Taylor SH, Wei W, Raber MN, Lenzi R and Abbruzzese JL. Metastatic patterns in adenocarcinoma. *Cancer* 2006; 106: 1624-1633.
- [8] Liede A, Jerzak KJ, Hernandez RK, Wade SW, Sun P and Narod SA. The incidence of bone metastasis after early-stage breast cancer in Canada. *Breast Cancer Res Treat* 2016; 156: 587-595.
- [9] Howat WJ, Warford A, Mitchell JN, Clarke KF, Conquer JS and McCafferty J. Resin tissue microarrays: a universal format for immunohistochemistry. *J Histochem Cytochem* 2005; 53: 1189-1197.
- [10] Ng ES, Kangarloo SB, Konno M, Paterson A and Magliocco AM. Extraction of tamoxifen and its metabolites from formalin-fixed, paraffin-embedded tissues: an innovative quantitation method using liquid chromatography and tandem mass spectrometry. *Cancer Chemother Pharmacol* 2014; 73: 475-484.
- [11] Feldman AT and Wolfe D. Tissue processing and hematoxylin and eosin staining. *Methods Mol Biol* 2014; 1180: 31-43.
- [12] Liu X, Shen M, Qi Q, Zhang H and Guo SW. Corroborating evidence for platelet-induced epithelial-mesenchymal transition and fibroblast-to-myofibroblast transdifferentiation in the development of adenomyosis. *Hum Reprod* 2016; 31: 734-749.
- [13] Zhu X, Cheng YQ, Du L, Li Y, Zhang F, Guo H, Liu YW and Yin XX. Mangiferin attenuates renal fibrosis through down-regulation of osteopontin in diabetic rats. *Phytother Res* 2015; 29: 295-302.
- [14] Wu H, Xie J, Li GN, Chen QH, Li R, Zhang XL, Kang LN and Xu B. Possible involvement of TGF-beta/periostin in fibrosis of right atrial appendages in patients with atrial fibrillation. *Int J Clin Exp Pathol* 2015; 8: 6859-6869.
- [15] Haisan A, Rogojanu R, Croitoru C, Jitaru D, Tarniceriu C, Danciu M and Carasevici E. Digital microscopy assessment of angiogenesis in different breast cancer compartments. *Biomed Res Int* 2013; 2013: 286902.
- [16] Schmid M, Dufner B, Durk J, Bedal K, Stricker K, Prokoph LA, Koch C, Wege AK, Zirpel H, van Zandbergen G, Ecker R, Boghiu B and Ritter U. An Emerging approach for parallel quantification of intracellular protozoan parasites and host cell characterization using TissueFAXS cytometry. *PLoS One* 2015; 10: e0139866.
- [17] Rogojanu R, Thalhammer T, Thiem U, Heindl A, Mesteri I, Seewald A, Jager W, Smochina C, Elinger I and Bises G. Quantitative image analysis of epithelial and stromal area in histological sections of colorectal cancer: an emerging diagnostic tool. *Biomed Res Int* 2015; 2015: 569071.
- [18] Stoffel E, Maier H, Riedl E, Bruggen MC, Reininger B, Schaschinger M, Bangert C, Guevova E, Stingl G and Brunner PM. Analysis of anti-TNF-induced skin lesions reveals strong Th1 activation with some distinct immunological characteristics. *Br J Dermatol* 2017.
- [19] Derricott H, Jones RL, Greenwood SL, Batra G, Evans MJ and Heazell AE. Characterizing villitis of unknown etiology and inflammation in stillbirth. *Am J Pathol* 2016; 186: 952-961.
- [20] Oskarsson T. Extracellular matrix components in breast cancer progression and metastasis. *Breast* 2013; 22 Suppl 2: S66-72.
- [21] Insua-Rodriguez J and Oskarsson T. The extracellular matrix in breast cancer. *Adv Drug Deliv Rev* 2016; 97: 41-55.
- [22] Kakkad SM, Solaiyappan M, Argani P, Sukumar S, Jacobs LK, Leibfritz D, Bhujwalla ZM and Glunde K. Collagen I fiber density increases in lymph node positive breast cancers: pilot study. *J Biomed Opt* 2012; 17: 116017.
- [23] Fu Z, Song P, Li D, Yi C, Chen H, Ruan S, Shi Z, Xu W, Fu X and Zheng S. Cancer-associated fibroblasts from invasive breast cancer have an attenuated capacity to secrete collagens. *Int J Oncol* 2014; 45: 1479-1488.
- [24] Brabrand A, Kariuki II, Engstrom MJ, Haugen OA, Dyrnes LA, Asvold BO, Lilledahl MB and Bofin AM. Alterations in collagen fibre patterns in breast cancer. A premise for tumour invasiveness? *APMIS* 2015; 123: 1-8.
- [25] Provenzano PP, Inman DR, Eliceiri KW, Knittel JG, Yan L, Rueden CT, White JG and Keely PJ. Collagen density promotes mammary tumor initiation and progression. *BMC Med* 2008; 6: 11.
- [26] Acerbi I, Cassereau L, Dean I, Shi Q, Au A, Park C, Chen YY, Liphardt J, Hwang ES and Weaver VM. Human breast cancer invasion and aggression correlates with ECM stiffening and immune cell infiltration. *Integr Biol (Camb)* 2015; 7: 1120-1134.